BREAKDOWN VOLTAGE EVALUATION OF HOMOGENEOUS INSULATING SYSTEMS WITH DIELECTRIC BARRIERS

Mona Ghassemi[1*], *Student Member, IEEE,* Hossein Mohseni[1], Kaveh Niayesh[1],
Senior Member, IEEE and Amir Abbas Shayegani[1]
High Voltage Lab., School of Electrical and Computer Engineering,
College of Engineering, University of Tehran, Tehran, Iran
*Email: m.ghassemi@ece.ut.ac.ir

Abstract: Discharge development mechanisms in solid/gas insulation systems with dielectric barriers are still not completely understood. Such insulating concepts can be used as an alternative for gas insulation systems (air or SF_6 and its mixtures) to enhance electrical insulation strength in high voltage apparatus. In this paper, a detail model of a homogeneous barrier discharge is developed to study the performance of mixed solid/gas insulating systems with dielectric barriers. For this purpose, electron transport is described based on the continuity equations for number density and mean energy density of electrons. For diffusive transport modeling of heavy particles (including ions, excited atoms and molecules and neutral atoms and molecules), the mixture-averaged evaluation is formulated and the aspects of plasma chemistry and surface reactions are taken into account. The model is based upon a simultaneous solution of all foregoing equations together with the Poisson's equation. The simulation results for applying a standard lightning impulse voltage is presented and discussed.

1 INTRODUCTION

Dielectric barrier discharge (DBD) is one of the important sources for nonequilibrium plasma generation in the atmospheric pressure with gas and ion temperature practically at room-temperature level [1]. Dielectric barrier discharges (sometimes referred to as silent discharge) that are ac discharge between two electrodes, with at least one intervening dielectric layer, are generally assessed as being of growing importance [2].

In the present time, the discharge at atmospheric pressure controlled by dielectric barriers has many applications, for instance, ozone generation, pollution control, medical and biological control, plasma display panels, thin-film deposition, surface modification and etching [3, 4].

However, it has not yet adapted to high-voltage insulation applications. In [5, 6], experimental results of DBD used to enhance the lightning impulse insulation strength have been reported. The DBD modeling in high voltage electric power applications has been mainly based on its static behaviour, taking into account the charges deposited on the dielectric surfaces and calculating the electric field in the gap [2, 7-9]. In [9], the effect of a conductor coating on the onset voltage of coronas on transmission-line conductors has been investigated.

Reference [10] presents a simple model based on Paschen's law and the breakdown voltage in uniform electric fields for air and space charges produced in DBD air gap. A model of the homogenous barrier discharge was developed in [11]. This model was based upon a simultaneous solution of the continuity equations for charged and excited particles, and the Poisson's equation across gap and dielectric coatings using explicit flux-corrected transport technique, developed mainly in [12].

In this paper, a precise model is presented to describe various steps of dielectric barrier discharge development. In the proposed model, free electrons and heavy species transport equations, plasma chemistry and surface reactions are simultaneously solved with Poisson's equations.

The proposed model allows us to study the structure of the homogeneous barrier discharges in detail. In particular, the spatio-temporal distributions of electric field and densities of charged particles are obtained. Such analysis helps us to better understand the processes proceeding in a discharge. For this purpose, the governing equations of the model are presented and solved. The simulation results indicate that the breakdown voltage of mixed solid/gas insulating systems can be significantly improved using appropriate dielectric barriers.

2 MODEL FORMULATION

The developed model here solves the free electron transport equations, the diffusive transport equations for heavy species, chemistry plasma and surface reaction formula simultaneously with Possion's equation.

2.1 Electron Transport Equations

The continuity equation for free electrons in gap is given by [13]

$$\frac{\partial n}{\partial t} + \nabla.\left(-\mu E n - \nabla(Dn)\right) = S, \qquad (1)$$

where n is the electrons number density, μ and D are the mobility and diffusion coefficient, E is the electric filed and S is the net electron source term.

Similar to the continuity equation, the energy equation is given by [13]

$$\frac{\partial n_\varepsilon}{\partial t} + \nabla.\left(-\mu_\varepsilon E n_\varepsilon - \nabla(D_\varepsilon n_\varepsilon)\right) + E.\left(-\mu E n - \nabla(Dn)\right) = S_\varepsilon, \qquad (2)$$

where n_ε is the energy density, μ_ε and D_ε are the energy mobility and diffusion coefficient and S_ε is the total energy transfer due to collisions.

2.2 Diffusive Transport Equations for Heavy Species

Neutral, excited species and ions in plasma require a suitable transport equation.

Suppose a reacting flow consists of $k = 1, \ldots, Q$ species and $j = 1, \ldots, N$ reactions. The equation for the first $Q - 1$ species is given by [14]

$$\rho\frac{\partial Y_k}{\partial t} + \rho(\mathbf{V}.\nabla)Y_k = \nabla.\mathbf{j}_k + R_k, \qquad (3)$$

where $\mathbf{j}_k$ is the multicomponent species flux, R_k is the rate expression for species, $\mathbf{V}$ is the mass averaged fluid velocity vector, ρ denotes the density of the mixture and Y_k is the mass fraction of species k. The mass average velocity $\mathbf{V}$ is defined as

$$\mathbf{V} = \frac{1}{\rho}\sum_{k=1}^{K} \rho_k \widetilde{\mathbf{V}}_k = \sum_{k=1}^{K} Y_k \widetilde{\mathbf{V}}_k, \qquad (4)$$

where $\widetilde{\mathbf{V}}_k$ is the average velocity of species k at a given location in the fluid relative the fixed laboratory frame of reference. This is not the velocity of individual molecules of species k but the average value over all species k molecules at this location in the fluid, ρ_k is the mass density of species k, and the mass fraction of species k is $Y_k = \rho_k/\rho$.

The diffusive flux vector is defined as

$$\mathbf{j}_k = \rho_k\left(\widetilde{\mathbf{V}}_k - \mathbf{V}\right) = \rho_k \mathbf{V}_k = \rho Y_k \mathbf{V}_k, \qquad (5)$$

where the mass diffusion velocities $\mathbf{V}_k$ are [15]

$$\mathbf{V}_k = \frac{1}{Y_k \bar{W}} \sum_{j=1,\neq k}^{K} W_j D_{kj} \mathbf{d}_j - \frac{D_k^T}{\rho Y_k}\frac{1}{T}\nabla T. \qquad (6)$$

The species molecular weights are denoted by W_j, the mean molecular weight by $\bar{W}$, and the temperature by T.

For low density, ideal gases, the diffusion driving force $\mathbf{d}_k$ is defined as

$$\mathbf{d}_k = \nabla X_k + \left(X_k - Y_j\right)\frac{1}{p}\nabla p, \qquad (7)$$

where X_k is the mole fraction of species k, and p is the pressure. Additional terms are introduced for interdiffusion of dense gases or liquids and $\mathbf{d}_k$ is generalized as [16, 17]

$$\mathbf{d}_k = \frac{1}{cRT}\left[\nabla p_k - Y_k \nabla p - \rho_k \mathbf{g}_k + \sum_{k=1}^{K} \rho_j \mathbf{g}_j\right], \qquad (8)$$

where $c = \sum_{k=1}^{K}[X_k]$ is the total molar concentration ($[X_k] = cX_k$ is the molar concentration), R is the universal gas constant, $\mathbf{g}_k$ is any (external) force per unit mass acting on species k, and ∇p_k is the "partial pressure gradient" for a non-ideal gas. The external force per unit mass is then given by

$$\mathbf{g}_k = \frac{Z_k F}{W_k} E, \qquad (9)$$

where Z_k is the charge number of species k, F is Faraday's constant and W_k is the molecular weight of species k.

The multicomponent diffusion coefficients D_{kj} and thermal diffusion coefficient D_k^T may be accurately computed from the solution of a system equation defined based on Chapman-Enskog theory and the presented technique in [15, 18]. However this technique requires some matrix inversion, hence we follow an approximation method known as the mixture-averaged evaluation in this paper. In this case, we desire to calculate D_{km} (i.e., a diffusion coefficient for diffusion of species k into a mixture of other gases). This can result in savings in computational cost.

For isothermal and isobaric conditions (i.e. $\nabla T = \nabla p = 0$), and assumption about the mass diffusion velocities $\mathbf{V}_k$ in terms of the mass fraction gradient,

$$\mathbf{V}_k = -\frac{1}{Y_k} D_{km}\, \nabla Y_k, \qquad (10)$$

an expression analogous to equation (6) for the mass flux $\mathbf{j}_k$ is given by (known as Fick's Law)

$$\mathbf{j}_k = \rho_k\left(\widetilde{\mathbf{V}}_k - \mathbf{V}\right) = \rho Y_k \mathbf{V}_k = -\rho D_{km} \nabla Y_k. \qquad (11)$$

With making the simplifying approximation that the velocities of all species $j \neq k$ are equal, the mixture-averaged diffusion coefficient D_{km} can be calculated from [19]

$$\frac{1}{D_{km}} = \sum_{j\neq k}^{K} \frac{X_j}{\mathcal{D}_{kj}} + \frac{X_k}{1 - Y_k}\sum_{j\neq k}^{K} \frac{Y_j}{\mathcal{D}_{kj}}, \qquad (12)$$

where $\mathcal{D}_{kj}$ are known as binary diffusion coefficients. In a low-density limit, from kinetic theory those are given as [15]

$$\mathcal{D}_{kj}\left[\frac{m^2}{s}\right] = 0.0188\frac{\sqrt{T^3/W_{kj}}}{p\sigma_{kj}^2 \Omega^{(1,1)*}\left(T_{kj}^*\right)}, \qquad (13)$$

where $W_{kj}(g/mol) = W_k W_j/\left(W_k + W_j\right)$ is the reduced molecular weight (W_k and W_j are molecular weight of species k and j, respectively), $T(K)$ is temperature, $p(N/m^2)$ is pressure, $\sigma_{kj}(\text{Å}) = \sigma_k \sigma_j/\left(\sigma_k + \sigma_j\right)$ is the reduced potential characteristic length, and the reduced collision integral $\Omega^{(1,1)*}(T_{kj}^{*})$ may be approximated by a fit as [15]

$$\Omega^{(1,1)*}(T_{kj}^{*}) = 1.0548 T_{kj}^{*-0.15504} + \left(T_{kj}^{*} + 0.55909\right)^{-2.1705}, \qquad (14)$$

where $T_{kj}^{*} = k_B T/\epsilon_{kj}$ is the reduced temperature (k_B is Boltzmann's constant) and is a function of the reduced potential well depth. For nonpolar species,

$$\frac{\epsilon_{kj}}{k_B} = \sqrt{\left(\frac{\epsilon_k}{k_B}\right)\left(\frac{\epsilon_j}{k_B}\right)}. \qquad (15)$$

However an alternative is to solve the Stefan-Maxwell equations in which the diffusion velocities are related *implicitly* to the field gradients [15, 20]:

$$\nabla X_k = \sum_{j=1}^{K} \frac{X_k X_j}{\mathcal{D}_{kj}}(\mathbf{V}_j - \mathbf{V}_k) + (Y_k - X_k)\left(\frac{\nabla p}{p}\right) + \sum_{j=1}^{K} \frac{X_k X_j}{\rho \mathcal{D}_{kj}}\left(\frac{D_j^T}{Y_j} - \frac{D_k^T}{Y_k}\right)\left(\frac{\nabla T}{T}\right). \qquad (16)$$

The set of K equations in equation (16) are not all independent. The equation set can be made unique by replacing one of the K equations with the constraint

$$\sum_{j=1}^{K} \mathbf{j}_k = \sum_{j=1}^{K} \rho Y_k \mathbf{V}_k = 0. \qquad (17)$$

The Stefan-Maxwell equations (16 and 17) form a system of linear equations that are solved for the K diffusion velocities $\mathbf{V}_k$. Even for isothermal and isobaric conditions, the Maxwell-Stefan equations quickly become computationally very expensive when the number of species becomes large. Also the fact that the chemical kinetics dominate a plasmas behaviour rather than diffusive transport, allows us to use a less stringent formulation of the Maxwell-Stefan equations.

2.3 Possion's Equations

The electric fields across gap and dielectric coatings are computed using Possion's equation:

$$-\nabla.\,\varepsilon_0 \varepsilon_r \nabla V = \rho \qquad (18)$$

where the space charge density, ρ is automatically computed based on the plasma chemistry specified in the model using the formula:

$$\rho = q\left(\sum_{k=1}^{N} Z_k n_k - n_e\right) \qquad (19)$$

where q is elementary charge.

The constitutive relation that describes the macroscopic properties of the dielectric coating medium (relating the electric displacement, D with the electric field, E) and the applicable material properties is given as

$$D = \epsilon_0 \epsilon_r E\,. \qquad (20)$$

Surface charge accumulation is added to boundaries by way of the following boundary condition:

$$-n.\,(D_1 - D_2) = \rho_s, \qquad (21)$$

where ρ_s is the solution of the following distributed ODE on the boundary:

$$\frac{d\rho_s}{dt} = \mathrm{n.J}_i + \mathrm{n.J}_e, \qquad (22)$$

where $\mathrm{n.J}_i$ and $\mathrm{n.J}_e$ are the normal component of the total ion current density and the total electron current density respectively on the wall.

2.4 Plasma Chemistry

The list of considered chemical reactions for Argon, as the gas filled in the gap, is as follows.

Table 1: Collisions and Modeled Reactions

React	Formula	Type	$\Delta\varepsilon(eV)$
1	$e + Ar \to e + Ar$	Elastic	0
2	$e + Ar \to e + Ars$	Excitation	11.5
3	$e + Ar^{*} \to e + Ar$	Superelastic	-11.5
4	$e + Ar \to 2e + Ar^{+}$	Ionization	15.8
5	$e + Ar^{*} \to 2e + Ar^{+}$	Ionization	4.427
6	$Ar^{*} + Ar^{*} \to e + Ar + Ar^{+}$	Penning ionization	---
7	$Ar^{*} + Ar \to Ar + Ar$	Metastable quenching	---

$\Delta\varepsilon(eV)$ is energy loss. A Maxwellian form is assumed for Electron Energy Distribution Function (EEDF). The cross section data for Argon is obtained from [21].

In addition to the volumetric reactions, the following surface reactions are implemented.

Table 2: Collisions and Modeled Reactions

Reaction	Formula
1	$Ar^{*} \to Ar$
2	$Ar^{+} \to Ar$

According to Table 2, when ions and excited atoms reach the wall, those are assumed to change back to neutral Argon atoms.

3 RESULTS AND DISCUSSION

Figure 1a shows the considered geometry for simulations including a small gap filled with Argon between two dielectric parallel plates. In this simple model the problem is reduced to one dimension by assuming the dielectric gap is much smaller than the diameter of the plates. A standard lightning impulse voltage ($1.2/50\ \mu s$) of positive polarity as follows is applied.

$$u(t) = 1.034U\left(e^{-t/\alpha_1} - e^{-t/\alpha_2}\right),$$

where $t(\mu s)$ is time, $1/\alpha_1$ and $1/\alpha_2$ are 68.2 and $0.405\ \mu s$ respectively [22], and $1.034U\ (V)$ is peak of the voltage amplitude. The voltage is applied on the upper dielectric (the point 1 in Figure 1b) whereas the lower one (the point 4 in Figure 1b) is grounded.

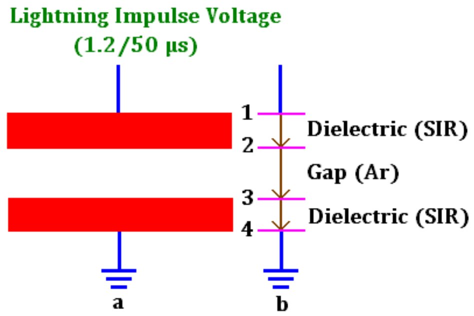

Figure 1: The considered geometry for simulations

The dielectric coatings are considered silicon rubber (SIR) with relative permittivity $\epsilon_r = 2.5$. The dielectric strength of the SIR is typically $20\ kV/mm$. Initially a small number of electron seeds $(10^6\ 1/m^3)$ is assumed to be present in gap. This amount is equal to typically around free electrons in air at sea level. Those are uniformly distributed in gap length with the initial mean energy 5 V. The initial number density of Argon ions is assumed the same initial density of electron seeds, $10^6\ 1/m^3$.

The peak of electrons and ions atoms number densities at the front of the impulse are given in Figure 2. The times when the impulse is 30% and 90% of crest value are 0.14 and $0.86\ \mu s$, repectively. The time for the voltage $u(t)$ to rise to its peak value (t_{max}) is $2.089\ \mu s$. From Figure 2 it can be seen that :

- Free electrons and Argon ions number densities peak in $0.5\ \mu s$ (at 70 % of crest value) when reach to 4.39×10^{18} and $4.69 \times 10^{18}\ 1/m^3$, respectively and then reamin nearly constant at peak to $1.0\ \mu s$ (at 90% of crest value) and then a gradual decrease to t_{max}.
- There is a dramatic rise in electrons and ions generation (i.e. considerable ionization activity) between 0.4 (at ~60 % of crest value) and $0.5\ \mu s$ whereas it is more sharply for electrons.
- The peak of densities with a plateau is around 70-90% of creast value and not at t_{max}. This is compatible with the measument results presented in [5, 10].

The Figures 3 and 4 show the free electrons number density and Argon ions number density in gap respectively, and Figures 5 and 6 show the voltage distribution and electric field across gap and coatings between 0.5 and $1.0\ \mu s$ (at 70-90% of crest value).

From Figure 2, it can be seen that the free electron concentration is near the dielectric coatings connected to high voltage with positive polarity. As the voltage applied to the upper plate increases, a stronger electric field forms in the gap between the plates. Any free electrons in the gap will be accelerated and since the electric field is strong enough they acquire enough energy to cause significant ionization activities as shown in Figure 3. Also an equal number of ions are also created and however due to be heavier than electrons, the ions are nearly the dielectric plate connected to high voltage as shown in Figure 4.

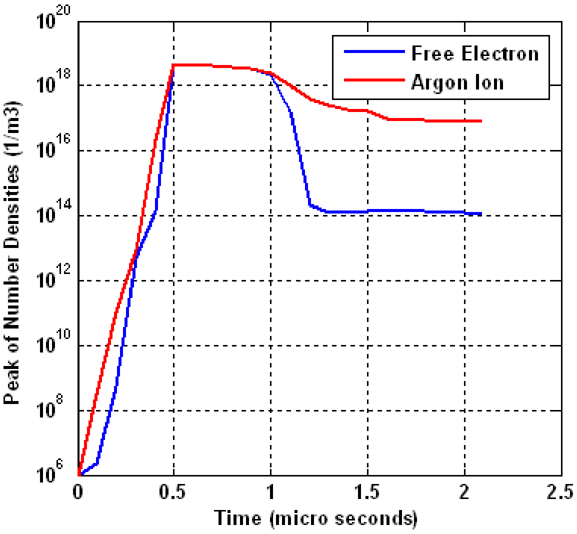

Figure 2: Peak of electrons and ions number densities at the front of the impulse

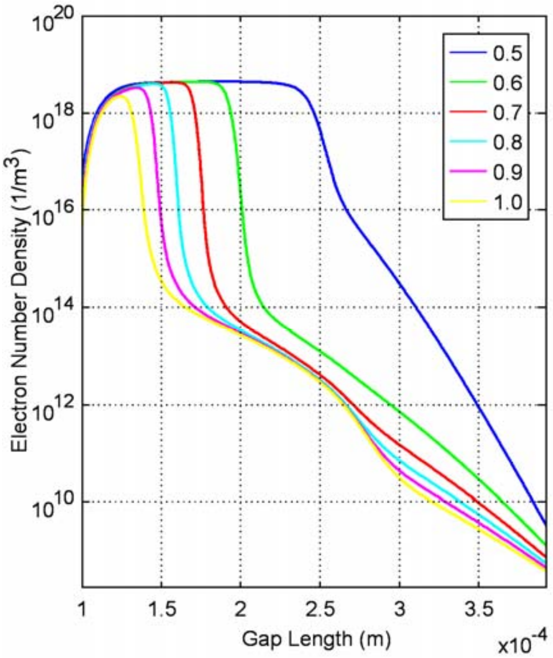

Figure 3: Electrons number densities at the front of the impulse

In initial times of applied impulse, there is not still enogth space charge to effect the electric filed and voltage distribution across gap. Hence there is the linear voltage distribution and uniformly electric filed based on capacitive properties (relative permittivity) of gap and coating not shown here. However at times between 0.5 and $1.0\ \mu s$, these densities increase dramatically and the voltage distribution and electric field across gap become nonlinear as shown in Figures 5 and 6. The more the densities is, the more nonlinearity impacts.

However in the following times this trend is mitigated and the electron density and ion number density are decreased and continue to the tail of impulse of course not shown here for brevity. In other hand, our simulation results show that the most activities of discharge including ionization and excitation processes occur at the front of impulse around 70-90% of creast value. However the maximum electric field in dielectric coatings is at the tail of the impulse during the voltage's decay.

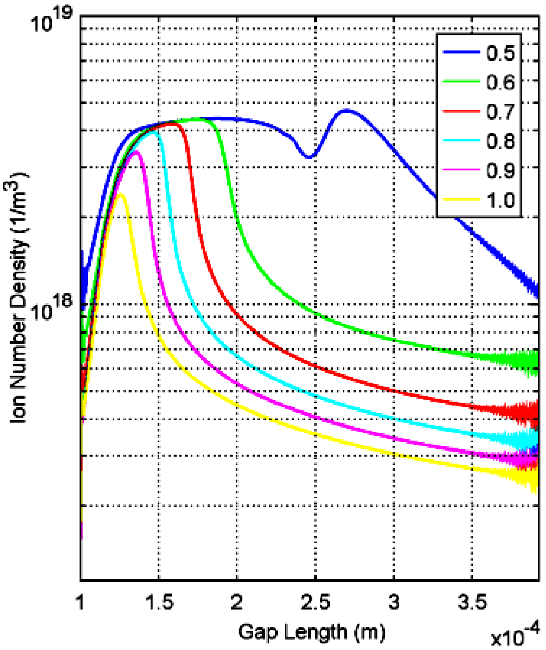

Figure 4: Ions number densities at the front of the impulse

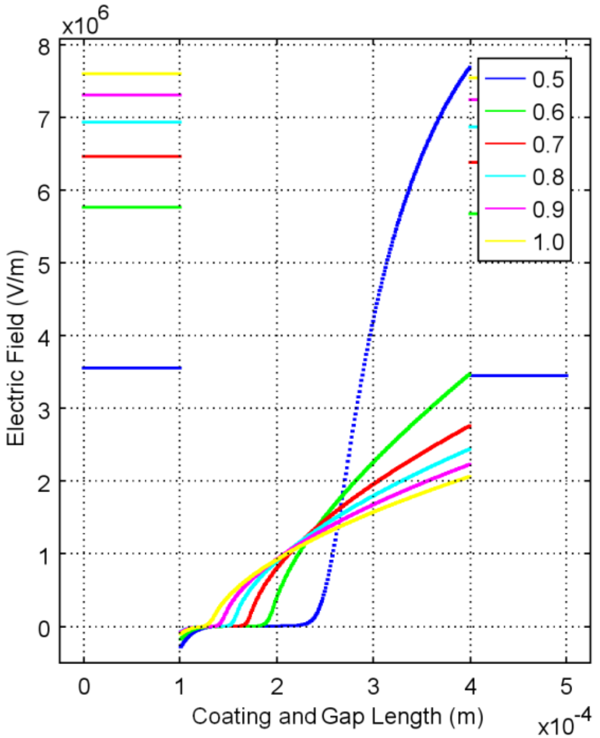

Figure 5: Electric field across gap and coatings at the front of the impulse

For the selected geometry here, it occurs in the dielectric coating connected to impulse voltage in around 7 μs that reaches to $9\ kV/mm$. This maximum amount is however less than the dielectric strength of the SIR which is typically $20\ kV/mm$.

Based on Paschen's law for uniform field electrode gaps, the breakdown voltage is given [23]

$$V_{br} = \frac{B(pd)}{\ln[(pd)A] - \ln\left[\ln\left(\frac{1}{\gamma}+1\right)\right]}, \qquad (20)$$

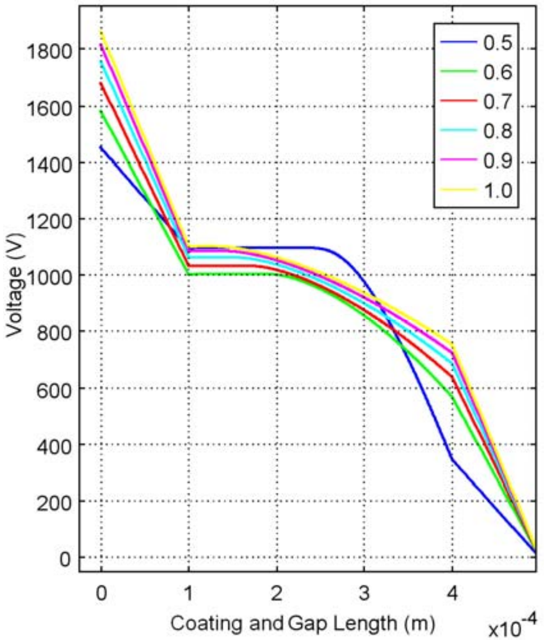

Figure 6: Voltage distribution across gap and coatings at the front of the impulse

where p is gas pressure, d is gas spacing, γ is the secondary ionization coefficient. Constants A and B for Argon are [23]

$$B = 235\ [V/torr.cm], A = 13.6\ [1/torr.cm].$$

About the considered example without dielectric coatings and with assumption gap (with length of 0.5 mm) filled up Argon and in atmosphere pressure (760 Torr), the breakdown voltage based on Paschen's law is $1.7036\,kV$ that is equals to an $3.3199\ kV/mm$ electric field. In the simulated example in this paper, the peak amplitude of impulse lightning ($2.068\,kV$) is considered more than the breakdown voltage without coatings and was showed that the maximum electric filed in dielectric coatings is still less than the dielectric strength of coatings.

Figure 7 shows the breakdown voltages for various thicknesses of coating and for positive and negative polarity of applied voltage. In all cases, total thickness of insulation set from high voltage electrode to grounded electrode is assumed $0.5\,mm$ and per cent of dielectric coating of insulation set n is given by

$$n = 100\frac{t_c}{(t_c + t_g) = 0.5\,mm},$$

where t_c is total thickness of dielectric coatings and t_g is gap thickness. The Percentage of insulation performance improvement is given by

$$m_{\pm} = 100\frac{|V_{br}^{\pm}| - V_{br1}}{V_{br1}},$$

where $V_{br}^{\pm}$ and V_{br1} are breakdown voltages with dielectric coating (applied voltage with positive and negative polarity) and without it, respectively.

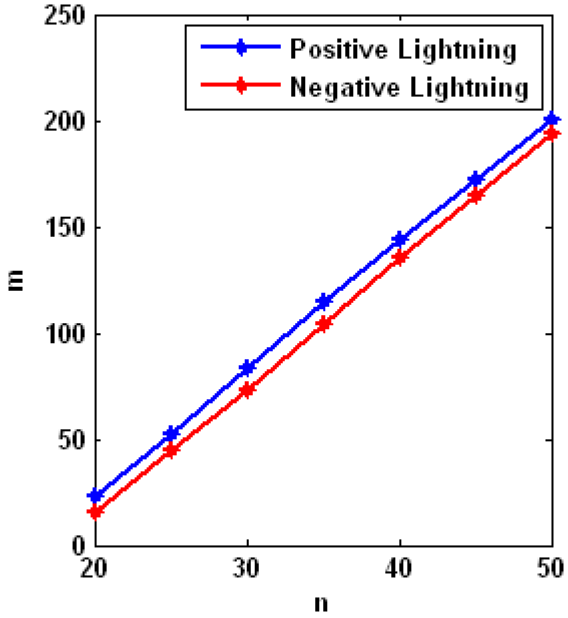

Figure 7. The breakdown voltages for various thicknesses of coating and for positive and negative polarity of applied voltage

According to Figure 7:

- If only 20 percent of gap thickness is coated by a dielectric, the insulation performance will be improved nearly 20% and with increasing the thickness of dielectric coatings until 40% and 50%, it will dramatically increase to nearly 140% and 200% respectively. Thanks for DBD.
- The breakdown voltages for negative polarity are a little more than it for the positive polarity.
- There is a steady improvement in insulation performance from 20 to 200% with increasing thickness of the dielectric coatings from 20 to 50%.

Also the simulations with unequal thickness of dielectric coatings are repeated. For the same total thickness of dielectric coatings, the breakdown voltages for unequal thickness are less than those for the equal thickness.

4 CONCLUSION

This paper develops a precise model to study the insulation performance improvement of DBD. The model is based on chemistry plasma, the electron and heavy species transport physics, and surface reactions. For electron transport modeling, the continuity equations for free electrons and their energies were solved accurately base on a Maxwellian EEDF and cross-section data for gas filled up in the gap. The transport phenomena for heavy species were modeled via a mixture-averaged formulation that is precise for DBD modeling. In chemistry plasma, we consider all existing reactions for the selected gas. It was showed that with increasing the dielectric coating thickness, a markedly overall better insulation performance would be resulted.

5 REFERENCES

[1] B. Eliasson and U. Kogelschatz: "Non-equilibrium Volume Plasma Chemical Processing", IEEE Trans. Plasma Sci., Vol. 19, pp. 1063–1077, 1991.
[2] H. J. Blennow, M. Sjoberg, M. A. S. Leijon, S. M. Gubanski: "Electric Field Reduction Due to Charge Accumulation in a Dielectric-Covered Electrode System", IEEE TDEI, Vol.7, No. 3, pp. 340–5, 2000.
[3] U. Kogelschatz, B. Eliasson, W. Egli: "From Ozone Generators to Flat Television Screens: History and Future Potential of Dielectric–Barrier Discharges", Pure Appl. Chem., Vol. 71, pp. 1819-1828, 1999.
[4] S. Mohapatro, B. S. Rajanikanth: "Cascaded Cross Flow DBD-Adsorbent Technique for NO_X Abatement in Diesel Engine Exhaust", IEEE TDEI, Vol. 17, pp. 1543–1550, 2010.
[5] H. J. Blennow, M. L. A. Sjoberg, M. A. S. Leijon, S. M. Gubanski, "Effect of Charge Accumulation in a Dielectric Covered Electrode System in Air", Conference on Electrical Insulation and Dielectric Phenomena, Austin, USA, 1999.
[6] F. Mauseth, A. Nysveen, E. Ildstad: "Charging of Dielectric barriers in rod-plane gaps", International Conference on Solid Dielectric, Toulouse, France, 5-9 July, 2004.
[7] M. Abdel-Salam, H. Singer, A. Ahmed: "On the Static Behavior of Dielectric Barrier Discharges in Uniform Fields", J. Phys. D: Appl. Phys., Vol.34, pp.1974–81, 2001.
[8] M. Abdel-Salam, H. Singer, A. Ahmed: "Effect of the Dielectric Barrier on Discharge in Non-Uniform Electric Fields", J. Phys. D: Appl. Phys., Vol.34, pp.1219–34, 2001.
[9] M. Abdel-Salam, A. A. Turky, A. Hashem: "The Onset Voltage of Coronas on Bare and Coated Conductors", J. Phys. D: Appl. Phys., Vol. 31, pp. 2550–6, 1998.
[10] H. J. Blennow, M. A. S. Leijon, S. M. Gubanski, "Active High Voltage Insulation", J. Electrostatics, Vol. 55, pp. 159–72, 2002.
[11] Y. V. Serdyuk, S. M. Gubanski: "Computer Modeling of Interaction of Gas Discharge Plasma with Solid Dielectric Barriers", IEEE TDEI, Vol. 12, No. 4, pp.725–35, 2005.
[12] R. Morrow, J. J. Lowke, "Streamer propagation in air", J. Phys. D: Appl. Phys., Vol.30, pp. 614–27, 1997.
[13] G. J. M. Hagelaar, L. C. Pitchford: "Solving the Boltzmann Equation to Obtain Electron Transport Coefficients and Rate Coefficient for Fluid Models", Plasma Sources Sci. Technol., Vol. 14, pp. 722–33, 2005.
[14] COMSOL Multiphysics, Plasma Module, April 2010.
[15] R.J. Kee, M.E. Coltrin, P. Glarborg: Chemically Reacting Flow Theory and Practice, Wiley, 2003.
[16] C.F. Curtiss, R. B. Bird: "Multicomponent Diffusion," Ind. Eng. Chem. Res., Vol. 38, pp. 2515-22, 1999.
[17] J. O. Hirschfelder, C. F. Curtiss, R. B. Bird: Molecular Theory of Gases and Liquids, John Wiley, New York,1954.
[18] G. Dixon-Lewis: "A FORTRAN Computer Code Package for the Evaluation of Gas-Phase Multicomponent Transport Properties," Proc. Royal Soc., Vol. A304, pp.111-35, 1968.
[19] R. B. Bird, W. E. Stewart, E. N. Lightfoot: Transport Phenomena, (2nd ed.), Wiley, 2002.
[20] J. C. Maxwell: "On the Dynamical Theory of Bases," Phil. Trans. Roy. Soc. London, Vol. 157, pp. 49-88, 1867.
[21] A. V. Phelps: ftp://jila.colorado.edu/collision_data/.
[22] E. Kuffel, W. S. Zaengl, J. Kuffel: High Voltage Engineering Fundamentals, Butterworth-Heinemann, 2000.
[23] N. Pedrow: Conduction and Breakdown in Gases-Part 1, http://193.140.122.139/high_voltage/pedrow/pedrow_hvoltage/index-18.html